SECOND-ORDER DIFFRACTION AND RADIATION SOLUTIONS ON FLOATING BODIES

By

C.-H. Lee and X. Zhu
Department of Ocean Engineering, MIT
Cambridge, MA 02139, USA

(Abstract for the 8th International Workshop on Water Waves and Floating Bodies, May 1993)

Summary

Computational results of the complete second-order solution for three dimensional bodies oscillating about their mean positions are presented. Green's integral equation is solved for the unknown second-order velocity potential on the body boundary. From the solution of this equation, the second-order pressure on the body and in the fluid domain, and the second-order wave elevation are computed. The forces obtained by direct pressure integration over the bodies are compared with those obtained by indirect approach using assisting potential.

Formulation

Following the notation of [1], $\mathbf{F}_p$ denotes the second-order potential force, $\Phi_I^{(2)}$ and $\Phi_S^{(2)}$ the second-order incident and scattered wave potentials, Q_B and Q_F the forcing on the body and free surface and $G(\mathbf{x};\boldsymbol{\xi})$ the Green's function of sum- or difference- frequency.

As is shown in [1], $\Phi_S^{(2)}$ on the body boundary is obtained as the solution of the following Green's integral equation,

$$2\pi\Phi_S^{(2)}(\mathbf{x}) + \iint_{S_B} \Phi_S^{(2)}(\xi)\frac{\partial G(\mathbf{x};\xi)}{\partial n_\xi}dS = \iint_{S_B} Q_B(\xi)G(\mathbf{x};\xi)dS + \iint_{S_F} Q_F(\xi)G(\mathbf{x};\xi)dS \qquad (1)$$

From the same equation, when 2π is replaced by 4π, we obtain $\Phi_S^{(2)}(\mathbf{x})$ in the fluid domain and on the free surface.

The second-order force is the sum of the quadratic force and $\mathbf{F}_p$ given by

$$\mathbf{F}_p = -\rho\iint_{S_B} \frac{\partial\Phi^{(2)}}{\partial t}\mathbf{n}dS. \qquad (2)$$

where $\Phi^{(2)} = \Phi_I^{(2)} + \Phi_S^{(2)}$, ρ is water density, and $\mathbf{n}$ denotes the normal vector out of fluid.

Finally, the second-order wave elevation $\eta^{(2)}$ is obtained from

$$\eta^{(2)} = -\frac{1}{g}\left(\frac{\partial\Phi^{(2)}}{\partial t} + \frac{1}{2}\nabla\Phi^{(1)}\cdot\nabla\Phi^{(1)} - \frac{1}{g}\frac{\partial\Phi^{(1)}}{\partial t}\frac{\partial^2\Phi^{(1)}}{\partial z\partial t}\right) \qquad (3)$$

Computational method

The major computational task for the second-order solution is the efficient and robust evaluation of the integrals on the right-hand-side of the equation (1).

Free surface integral:

In our earlier works ([1] and [2]), we divide the free surface into two regions separated by a partion circle 'b'. The radius of 'b' is large enough so that we may neglect the evanescent modes in the outer region.

In outer region of the free-surface, both Green function and the first-order potentials are expanded in Fourier-Bessel series. Due to the oscillatory behaviour of the Bessel functions with respect the order, the series is slowly convergent for large values of wavenumber and 'b'. The number of terms retained in the series increases with the wavenumber and 'b' and should be determined carefully. It is necessary to include up to the order of 64 in our computation for a typical tension-leg platform (TLP). After integrating the trigonometric functions with respect to the angular coordinates, the free-surface integral reduced to summations of line integrals in radial coordinates which are evaluated based on the adoptive numerical integration in complex plane as is described in [1].

In the inner region, the free surface is discretized with panels and the mid-point rule is applied using the value at the centroid of each panel. The integrand of free surface integral is, especially at sum frequency, highly oscillatory with several dominant frequencies (the existing quadratures for the highly oscillating functions are in general developed for a single dominant frequency). Due to this property of the integrand and the required large radius of 'b' as the water depth increases, the number of panels on the free surface can easily reach O(10000). As an effort to reduce the computational burden, we further subdivide the inner region into two parts separated by a circle of radius 'a' which barely encloses the bodies. The free-surface inside this circle is discretized with panels as before. Outside this circle, in the annulus between the circles of radii of 'a' and 'b', we adopt Gauss-Chebyshev quadrature in the azimuthal direction and Gauss-Legendre quadrature in the radial direction.

Body surface integral:

For floating bodies, the normal velocity on the mean body boundary, Q_B, is substantially more complicated than that of the first-order. As is derived in [3], it takes a form

$$Q_B = -\frac{\partial \Phi_I^{(2)}}{\partial n} + \mathbf{n}\cdot\frac{\partial H}{\partial t}\mathbf{r} + (\boldsymbol{\alpha}^{(1)}\times\mathbf{n})\cdot\left(\frac{\partial(\boldsymbol{\xi}^{(1)}+\boldsymbol{\alpha}^{(1)}\times\mathbf{r})}{\partial t} - \nabla\Phi^{(1)}\right) - \mathbf{n}\cdot((\boldsymbol{\xi}^{(1)}+\boldsymbol{\alpha}^{(1)}\times\mathbf{r})\cdot\nabla)\nabla\Phi^{(1)} \quad (4)$$

where $\boldsymbol{\xi}$ and $\boldsymbol{\alpha}$ are the translational and rotational displacements, respectively. H is a matrix containing the quadratic contribution of $\boldsymbol{\alpha}$ to the rotational matrix. The first term of equation (4) leads to the second-order scattered potential for fixed bodies and the rest of Q_B is associated with the motion of the body. The accurate evaluation of the double spacial derivative on the body surface in the last term may be difficult when we use the low order panel method. Instead, we recast the body surface integral involving double derivatives into the following form using various vector differential formulas:

$$\iint_{S_B} G\{\mathbf{n}\cdot[(\boldsymbol{\xi}^{(1)}+\boldsymbol{\alpha}^{(1)}\times\mathbf{r})\cdot\nabla]\nabla\Phi^{(1)}\}dS =$$

$$\iint_{S_B} [\mathbf{n}\cdot(\boldsymbol{\xi}^{(1)}+\boldsymbol{\alpha}^{(1)}\times\mathbf{r})](\nabla\Phi^{(1)}\cdot\nabla G)+G\{\mathbf{n}\cdot[(\nabla\Phi^{(1)}\cdot\nabla)(\boldsymbol{\xi}^{(1)}+\boldsymbol{\alpha}^{(1)}\times\mathbf{r})]\}$$

$$-\frac{\partial\Phi^{(1)}}{\partial n}[(\boldsymbol{\xi}^{(1)}+\boldsymbol{\alpha}^{(1)}\times\mathbf{r})\cdot\nabla G]+\mathbf{n}\cdot\{\nabla\times[\nabla\Phi^{(1)}\times G(\boldsymbol{\xi}^{(1)}+\boldsymbol{\alpha}^{(1)}\times\mathbf{r})]\}dS \qquad (5)$$

The last integral can be replaced by a line integral along the waterline by Stokes theorem.

$$\iint_{S_B}\mathbf{n}\cdot\{\nabla\times[\nabla\Phi^{(1)}\times G(\boldsymbol{\xi}^{(1)}+\boldsymbol{\alpha}^{(1)}\times\mathbf{r})]\}dS=\int_{WL}G[\nabla\Phi^{(1)}\times(\boldsymbol{\xi}^{(1)}+\boldsymbol{\alpha}^{(1)}\times\mathbf{r})]\cdot d\mathbf{l} \qquad (6)$$

Computational results

The numerical examples illustrating techniques for the free surface integrals are for the Snorre TLP with four columns of radius $a = 12.5m$, spacing $76m$ between column axes, and draft 37.5m. In Figure 1a, we plot the integrand of the free-surface integral along the circle of radius $300m$. The first-order incident wave frequencies are $\omega_1 = \omega_2 = 1.325$. Figure 1b shows the convergece of the integration using Gauss-Chebyshev quadrature. Figure 2a shows the variation of the integrand in radial direction between $100m$ to $300m$ after the integration in angular coordinate. As is shown in Figure 2b there are several dominant frequencies in the vicinity of the linear combinations wavenumbers of two first-order incident waves and an assisting potential. Table 1 shows the comparison between Romberg integration and Gauss quadrature for three different combinations of the first-order incident wave headings.

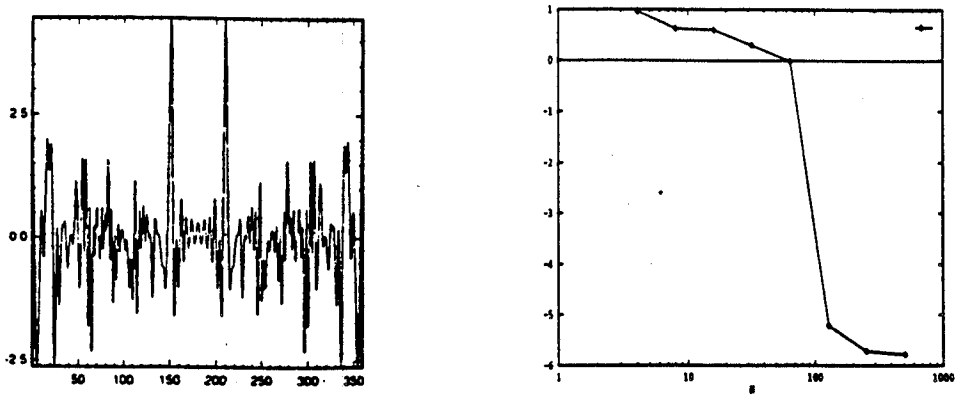

Figure 1a and 1b. Variation of the free-surface integrand in angular coordinate and the relative error of the integrated value.

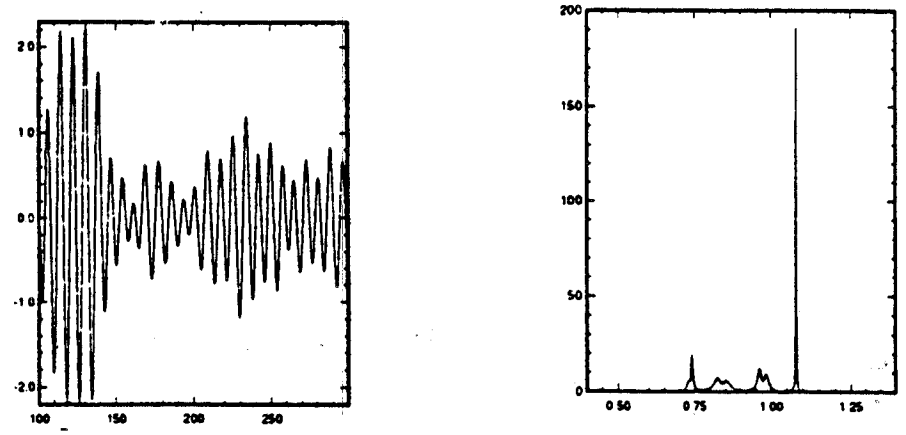

Figure 2a and 2b. Variation of the free-surface integrand in radial coordinate and it's Fourier component.

N	Romberg			N	Gauss		
$\beta_{1,2}$	0 0	0 45	0 90		0 0	0 45	0 90
257	334.44	66.72	294.50	53	754.00	2457.29	1508.29
513	335.04	62.42	290.84	65	334.88	62.54	290.78
1025	335.05	62.43	290.82	75	334.96	62.39	290.81

Table 1 Comparison between Romberg and Gauss-Legendre. β is wave heading and N is number of points computed between $100m$ to $300m$.

The second-order surge and heave forces on a floating hemisphere of radius $a = 1$ in water of depth 3 are computed by direct and indirect approach and compared with the result in [4]. Integration over the free-surface is performed by the mid-point rule. Partition radius $b = 3$ and 400 panels and 1800 panels are distributed on one quadrant of the body and the free surface, respectively. The heave force for Ka= 1.2 and 1.6 is significantly affected by the effect of the irregular frequency.

Additional computational results for a hemisphere and for a TLP will be presented at the workshop.

				Surge					
Ka	1.2			1.4			1.6		
1.2	1.108	1.078	1.067	1.035	0.977	0.948	0.980	0.910	0.879
1.4				0.974	0.899	0.857	0.924	0.843	0.806
1.6							0.888	0.801	0.778
				Heave					
Ka	1.2			1.4			1.6		
1.2	2.262	2.191	2.338	1.841	1.798	1.866	0.871	1.800	1.632
1.4				1.617	1.451	1.516	1.397	1.341	1.372
1.6							1.384	1.335	1.383

Table 2 Second-order forces on a floating hemisphere. Upper matrix is the surge forces and lower matix is the heave forces. First columns are forces by indirect approach, the second by direct approach and the third from [4].

Acknowledgement

The work is supported by the Joint Industry Projects 'Wave effects on offshore structures.' The development of the code and the computations were substantially facilitated by a Grant for the use of the Cray Y-MP and C90 at the Pittsburgh Supercomputer Center, with support from the National Science Foundation.

References

[1] Lee C.-H., Newman J.N., Kim M.-H. & Yue D.K.P. 1991 'The computation of second-order wave loads', OMAE, Stavanger, Norway

[2] Newman J.N. & Lee C.-H. 1992 'Sensitivity of wave loads to the discretization of bodies.' Conf. on the Behaviour of Offshore Structures (Boss '92), London.

[3] Ogilvie T. F. 1983 'Second-order hydrodynamic effe ts on ocean platforms.' Proceedings of the International Workshop on Ship and Platform Motions, Berkeley, pp 205-265

[4] Kim M.-H. & Yue D.K.P. 1990 ' The complete second-order diffraction solution for an axisymmetric body Part 2. Bichromatic incident waves and body motions.' *J. Fluid Mech.*, **211**, 557-593.